Electric Power Systems Research 184 (2020) 106324

Contents lists available at ScienceDirect

Electric Power Systems Research

journal homepage: www.elsevier.com/locate/epsr

The actual measurement and analysis of transformer winding deformation fault degrees by FRA using mathematical indicators

Ni Jianqiang[a], Zhao Zhongyong[a,*], Tan Shan[a], Chen Yu[a], Yao Chenguo[b], Tang Chao[a]

[a] College of Engineering and Technology, Southwest University, Chongqing 400716, China
[b] State Key Laboratory of Power Transmission Equipment & System Security and New Technology, Chongqing University, Chongqing 400044, China

ARTICLE INFO

Keywords:
Power transformer
Winding deformation
FRA
Numerical indices

ABSTRACT

Since the power transformers are indispensable in power systems, their reliable operation are of significance. Winding deformation is one of the most common failures within transformers. At present, many methodologies have been proposed to detect these faults, and frequency response analysis (FRA) technique is most frequently used because of its low cost, convenience, simplicity and effectiveness. However, there is no standard and reliable code to interpret the mechanical deformations from FRA traces as so far. In this study, an actual transformer experimental platform was used to simulate variable winding deformation faults in order to standardize the interpretation of winding fault degree from FRA data. The measured FRA raw data are processed from the perspective of statistics, and some numerical indices are found to be more suitable for the diagnosis of transformer winding deformation degree.

1. Introduction

The stable, reliable, safe and high quality power supply concerns the lives of hundreds of millions of people. As one of the most important pieces of equipment in power system, the stable operation of power transformer plays a critical role in the safe operation of the power system [1,2]. Statistics indicates that 25 percent of transformer faults were caused by winding mechanical deformation. Since the low voltage impulse (LVI) method was first introduced by Lech and Tyminski from Poland in 1966, many methodologies have been successively proposed to detect transformer winding deformation, for instance, the short circuit impedance (SCI) method, frequency response analysis (FRA) method and vibration method. SCI is based on the comparison and analysis of two short circuit impedance tests. In FRA, the frequency response traces are compared with its fingerprint to diagnose the occurrence of internal faults within power transformers. The vibration diagnosis method utilizes the characteristics that the transformer tank vibration will change when the winding fails [3]. Recently, some scholars present other improved techniques, namely, the sweep frequency impedance (SFI) method, which is the combination of SCI and FRA [1], the online impulse frequency response analysis (online IFRA) [4], the electromagnetic wave method [5] and the Lissajous locus method [6].

Above all, FRA is an effective and economic diagnostic technique for detection of mechanical deformations inside a power transformer [7]. FRA is sensitive to failures in the windings and iron core. What's more, it can provide reliable information about the geometry of active parts of the power transformer without any needs to dismantle the unit. FRA uses input voltage as the input signal and another voltage measured at the other terminal of transformer winding as the output signal, besides, the measured current could also be used as output signal. In most cases, the output voltage is used. However, a standard and widely accepted code for interpretation of FRA traces can be improved; at present, experienced personnel are still needed to diagnose winding faults by using visual inspection [8], which is still a matter of great concern.

At present, there are variable FRA interpretation methods, for instance, the equivalent electric model simulation method [9], the artificial intelligence method [10], and the mathematical statistics method [11]. In the first method, finite element analysis (FEA) of transformer winding is often used to build its equivalent electric model [12], to aid in interpreting the FRA curves. N. Hashemnia has studied the impact of winding axial displacement and radial deformation fault on equivalent electric parameters and FRA curves based on FEA [8,13], to improve the detection of winding faults. Besides, Z. W. Zhang has built a hybrid model based on FEA and multi-transmission line (MTL) to study the FRA curve beyond 1 MHz [14]. In the artificial intelligence method, M. Bigdeli has applied support vector machine (SVM) algorithm to classify the winding faults [15]. O. Aljohani et al. have introduced a novel FRA

* Corresponding author.
E-mail address: zhaozy1988@swu.edu.cn (Z. Zhao).

https://doi.org/10.1016/j.epsr.2020.106324
Received 19 April 2019; Received in revised form 30 January 2020; Accepted 7 March 2020
Available online 24 March 2020
0378-7796/

interpretation approach to detect transformer winding short-circuit fault, radial deformation and bushing faults by using polar plot and digital image processing [16], in which the various image unique features of a polar plot are extracted to construct diagnostic metrics. Artificial neural network (ANN) algorithm combined with cross-correlation features have also been used to discriminate between electrical and mechanical defects [17]. Of above methods, the third method, mathematical statistics method is often used due to its simplicity and accuracy. In this method, a number of numerical indices are proposed for the interpretation. E. Rahimpour has comprehensively compared the indices of frequency and amplitude deviation, standardized difference area, weight functions and other indices to evaluate the winding radial, axial and inter-turn fault [18]. The recently used statistical indicators have been summarized by Samimi in [11].

However, there still exists a problem regarding the application of mathematical indices. The transformer winding fault types can be roughly diagnosed because different frequency range of FRA trace is dominated by different active part of transformer. But for interpretation of transformer winding fault degrees, there exist a number of statistical indices which can be used. It is still unknown which indices are more suit for processing the fault degrees of specific fault types. To solve this problem, numbers of FRA traces of different winding fault types and degrees were obtained by artificial fault emulation on a specifically manufactured model transformer, which is reported in our previous study [19]. The measured FRA traces were analyzed in three sub-frequency bands to discover the characteristics of each fault type. Further, many mathematical indices between the FRA traces of normal conditions and failure conditions were calculated. In order to find the suitable indices for each failure situation, the sensitivity, relativity and monotonicity of each mathematical indicator are used as the evaluation criteria.

The remainder of this manuscript is organized as follows. First, the basic principle of FRA method is introduced in section II. Then, section III proposes the measurement setup and result of transformer winding deformation fault emulated experiment, followed by a frequency response analysis based on the mathematical statistical indicators in section IV. The conclusions of this study are introduced in last section.

2. Frequency response analysis

Studies have shown that the effect of transformer core can be ignored when the frequency exceeds 1000 Hz, the winding of a transformer can be equivalent to a two-port network comprising resistors, capacitors, and inductors, as shown in Fig. 1. The resistance is usually small and negligible. The internal properties of equivalent electric circuit can be expressed as its transfer functions $H(j\omega)$. The frequency response of the corresponding equivalent circuit will change as a mechanical fault happens within the transformer. Variations usually manifest themselves as changes in the shape of the frequency response, especially the resonant frequencies and the amplitudes. The variations between these frequency responses can potentially reveal the severity and type of failure, which is the main principle of FRA methods.

Due to the different ways of input signals, the test methods can be divided into sweep frequency response analysis (SFRA) method and impulse frequency response analysis (IFRA) method, and the SFRA is most frequently used [20,21]. In SFRA, the transformer to be investigated is taken out-of-service. Then a low voltage AC signal $U_1(j\omega)$ with sweep frequency is applied to one terminal of a transformer

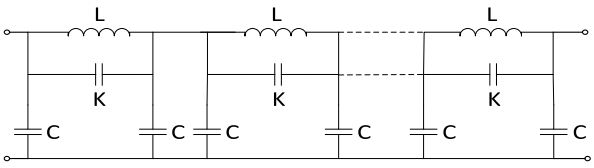

Fig. 1. Electric circuit of single phase transformer winding.

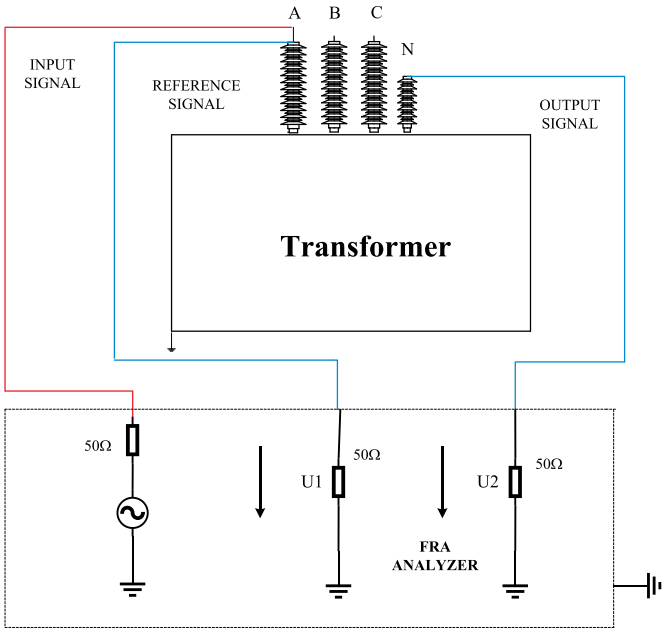

Fig. 2. Frequency response analysis end to end configuration.

winding and the response $U_2(j\omega)$ at the other terminal with reference to the earthed tank is measured. This is the basic test procedure of SFRA method. The transfer function $H(j\omega)$ can be expressed as:

$$H(j\omega)=\frac{U_2(j\omega)}{U_1(j\omega)} \tag{1}$$

The amplitude of $H(j\omega)$ is mostly considered and used, and it can be expressed in logarithmic form:

$$H(f) = 20\log\frac{|U_2(f)|}{|U_1(f)|} \tag{2}$$

The FRA testing equipment can be connected to the transformer in different ways, but the end-to-end connection, as shown in Fig. 2, is the mostly practical because the wiring is simple and the main types of mechanical faults can be detected by this way [20].

The Chinese standard DL/T 911–2004 [22] uses the sweep signals ranging from 1000 Hz to 1 MHz, while the IEC standard [23] suggests that the sweep frequency ranging from 20 Hz to 2 MHz is appropriate. The analysis indicates that the frequency band of a frequency response curve higher than 1 MHz is susceptible to the test leads, external interference, and the repeatability of FRA curve is not enough high. Therefore, the frequency band below 1 MHz is often taken as the test and analysis frequency band. The boundaries between the bands are widely discussed. The Chinese standard divides 1–1000 kHz into three parts, the low frequency band (1~100 kHz), the medium frequency band (100~600 kHz) and the high frequency band (600~1000 kHz). This definition has been widely used for FRA curves evaluation and has been adopted in the present work. In the low frequency band, the FRA curve is usually dominated by the inductive component due to flux penetration to the core. In the high frequency band, the most important factor affects the frequency response is the capacitive component, as the effect of this component is more significant as frequency increases. In the middle frequency band, both the capacitive and inductive components have influences on the frequency response. Therefore, the sensitivity of FRA curve to different faults in sub-frequency band is diverse. Generally speaking, the low frequency range of FRA curve is sensitive to core deformation, shorted turns and residual magnetism. The middle frequency band is sensitive to the deformation fault of the main winding, while in high frequency band, the FRA curve is sensitive to the faults that are the variations of grounded distribution capacitance.

3. Measurement of transformer winding deformation based on frequency response method

3.1. Introduction to experimental platform

In order to carry out the analysis based on mathematical statistics method, the FRA data of actual transformer winding deformations should be obtained at first. In our previous study [7, 19], a specially manufactured transformer was built up and used for winding deformation fault simulation tests, a large number of tests have been carried out on this specially manufactured model transformer. The inner part of the transformer is designed according to the structure of a 110 kV power transformer, and the transformer is the core type. The high-voltage winding is designed as a disk type winding. There are 30 disks in the single phase. 10 disks winding at the top and bottom are ordinary entanglement winding, 10 disks in the middle are sequential winding. The middle 10 disks winding are actually made as 5 groups of double disk type winding. Low-voltage winding is designed as layer type winding, which consists of six layers. The model transformer is shown in Fig. 3. The nameplate parameters are shown in Table 1.

In order to realize the purpose of detecting the winding short-circuit fault, winding radial deformation fault and disk space variation fault by frequency response method, in addition, the reusability of experimental facilities and experimental economy must be considered, the following modifications are performed to simulate various types of winding faults.

Winding inter-disk short circuit fault (SC): The connecters of the middle five sets of double cakes winding are numbered 1, 2, 3, 4, 5, and 6 from top to bottom. A short wiring is used to simulate the short circuit fault with different fault degree and fault locations, in which two terminals of wiring are connected to two connectors of middle windings, respectively. The actual image of this test is shown in Fig. 4. Then the FRA measurements of inter-disk short circuit experiments are carried out on model transformer.

Winding radial deformation fault (RD): In this experiment, we replaced the intermediate 10 high-voltage winding disks with the radial deformation windings of different deformation degrees and directions to simulate the winding radial deformation fault. The schematic diagram of radial deformed winding is shown in Fig. 5. The radius of winding is r, the degree of radial deformation part is represented by d, and the angle of deformation corresponding position is θ. In this experiment, θ is fixed at 45° and the angle difference between radial deformed parts is 90°. These special windings include four different types of radial deformation in one direction, two directions, three directions and four directions. Two groups of experiments were carried out: one disk deformed radially in the one direction, but the degree of deformation was different; the degree of deformed part was the same, but the number of radial deformed directions was different.

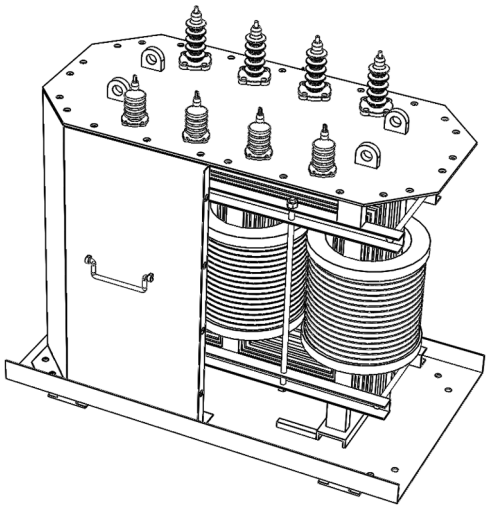

Fig. 3. Physical model of transformer.

Table 1
Design specifications of specifically manufactured model transformer.

Parameters		Nominal value
Rated voltage (kV)		10/0.4
Capacitance (pF)		400
Rated current (A)		23/557
Frequency (Hz)		50
Number of phase		3
Connection type		Ynyn0
Tank (mm)		1705 × 740 × 1415
HV winding	Outer radius (mm)	250
	Inner radius (mm)	210.5
	Height (mm)	519
LV winding	Out radius (mm)	174.5
	Inner radius (mm)	158
	Height (mm)	363
Iron core	Yoke radius (mm)	150
	Yoke height (mm)	1190
	Yoke length (mm)	1390

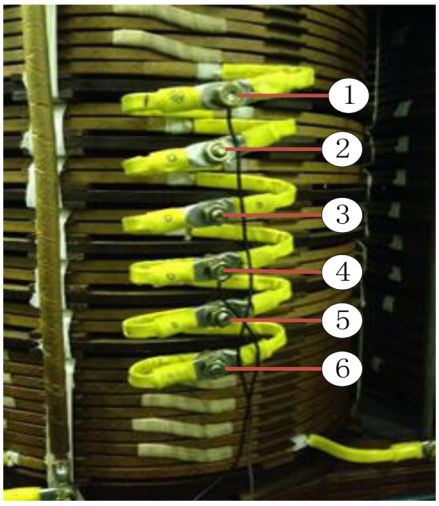

Fig. 4. Image of simulated short circuit fault experiment.

Disk space variation fault (DSV): Disk space variation fault mainly presents in the variation of the distance between the two adjacent disks. Considering that the variation of the distance between the disks mainly affects the capacitance between disks, it is feasible to simulate this type of fault by paralleling a capacitor between the disks. In this type of experimental setup, the connector numbers are identical with those of the short circuit experiment. Then the capacitors are connected in parallel between the two adjacent connectors, and the experiments of same paralleled capacitor with different parallel position and the experiments of same paralleled position with different parallel capacitors are carried out, respectively, to simulate different fault locations and degrees.

The test equipment is an FRA analyzer with product model of TDT6U, which adopts the linear sweep frequency method. Fig. 6 shows the schematic diagram of the wiring. Fig. 7 shows the image of actual experimental site.

3.2. Experimental results and spectrogram analysis

3.2.1. Winding inter-disk short circuit fault

In this group of experiments, frequency response of transformer under short circuit of connector number 1–6 is tested, respectively. Frequency response curves of short circuit fault with different degrees

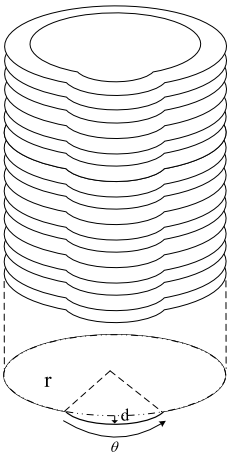

(a) Diagram of Radial Deformation of Winding

(b) Radial deformation in one direction

(c) Radial deformation in two directions

(d) Radial deformation in three directions

(e) Radial deformation in four directions

Fig. 5. Sketch of winding radial deformation.

are measured. FRA curves with different short circuit fault degrees are shown in Fig. 8.

It can be seen from Fig. 8 that compared with the frequency response in the normal state, the frequency response of the transformer in which the winding short-circuit fault occurs has a resonance point shifted in the low frequency band, and the amplitude of the resonance point has a large attenuation. In the middle frequency band, the degree of the resonance point shift increases as the degree of short circuit increases, while in the high frequency band, the spectral curve is severely distorted. Winding short-circuit faults mainly change the number of units in the equivalent circuit model of winding, and further change the inductance and capacitance parameters, which results in the variation of frequency response in each frequency band.

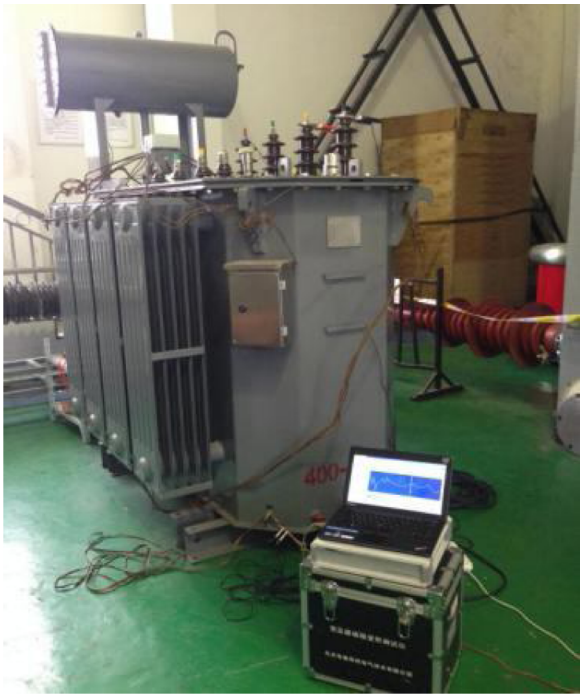

Fig. 7. Image of actual experimental site.

3.2.2. *Winding radial deformation fault*

In the first group, the first normal winding in the middle is replaced by a winding with one radial deformation direction, 3%, 5%, 7% and 10% deformation degrees, respectively. In the second group, the first normal winding in the middle is replaced by a winding with 5% deformation degree but with one, two, three and four radial deformation directions, respectively. Figs. 9 and 10 are the frequency response curves of the above two groups of experiments, respectively.

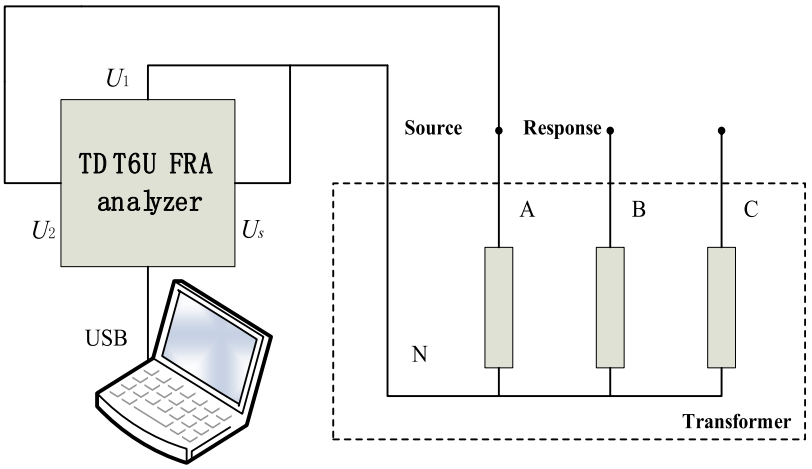

Fig. 6. Schematic diagram of transformer winding deformation experimental wiring.

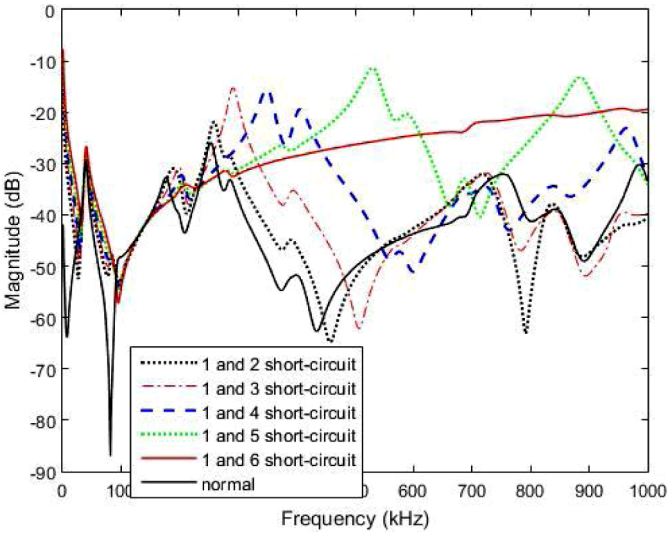

Fig. 8. Frequency response curves of short circuit fault with different degrees.

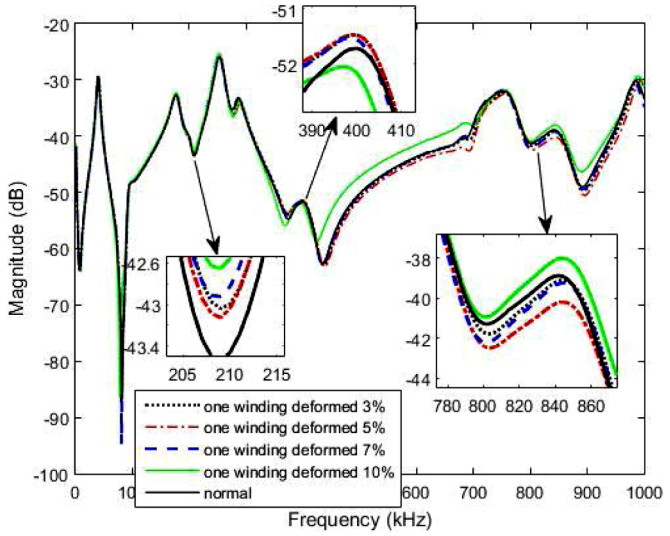

Fig. 9. Frequency response curve of different fault degree of radial deformation on a winding with the same fault direction.

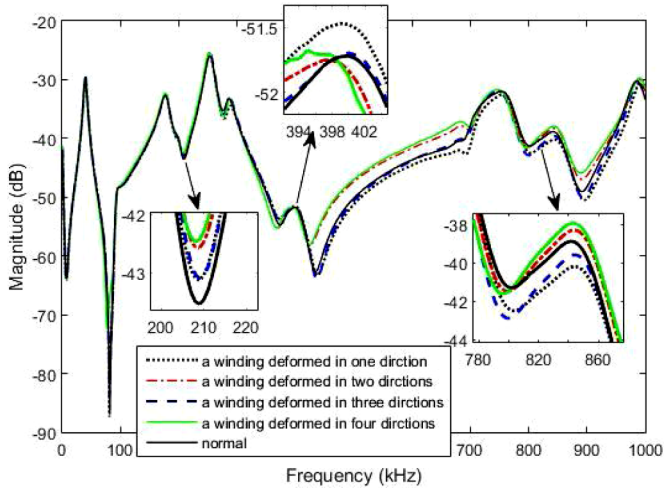

Fig. 10. Frequency response curve of different fault deformation on a winding with the same degree of deformation.

It can be seen from Fig. 9 that the difference between the frequency response under the fault state and that under the normal condition is small, and the frequency response curve under the fault state only changes slightly in the middle and high frequency band above 400 kHz. The situation in Fig. 10 is similar to that in Fig. 9. The radial deformation of windings essentially changes the ground capacitance of the equivalent circuit model of windings. It is discovered by many literatures that this type of fault mainly affects the middle and high frequency band of frequency response. From the two figures, the relationship between the offset degree of resonant frequency, magnitude and the direction of the radial deformation has not been directly found.

3.2.3. Disk space variation fault

For emulating this type of fault, two groups of experiment were also performed. In first group of experiment, we measured the frequency response of the winding when the capacitors of 50 pF, 100 pF, 200 pF, 400 pF, 600 pF and 800 pF were connected in parallel between the 1st and 2nd connectors, respectively, to simulate different fault degree with same fault location. In second group of experiment, we measured the frequency response of the winding when the capacitors of 150 pF was connected in parallel between the 1st and 2nd connectors and between the 3rd and 4th connectors, and between the 5th and 6th connectors, respectively, to simulate different fault location with same fault degree. The adjacent two disks of the healthy transformer were calculated based on FEM method, which is about 2000 pF. Thus, the capacitors with these capacitance values were selected, to simulate the fault degrees of 2.5%~40%. Frequency response curves of different fault degrees and locations are shown in Figs. 11 and 12, respectively.

From Fig. 11, it can be found that this type of fault has little effect on the low frequency band of the frequency response curve, while the resonant frequency in the medium and high frequency band decreases. It is noted that the amplitude of the resonances also change significantly in the high frequency band, especially for large paralleled capacitance. The changing trends of Figs. 11 and 12 are consistent with the trends of FRA curves described in [21], which demonstrates the feasibility of emulating DSV fault. Besides, in this experiment, it can be found that the variation of the amplitude of the resonance seems to have some correlation with the value of the paralleled capacitor. In Fig. 12, because the paralleled capacitance is small, the shift of resonance in the middle frequency band of faulty FRA curve is not obvious. In addition, the relationship between the different experimental FRA curves and the fault location is still not directly observable.

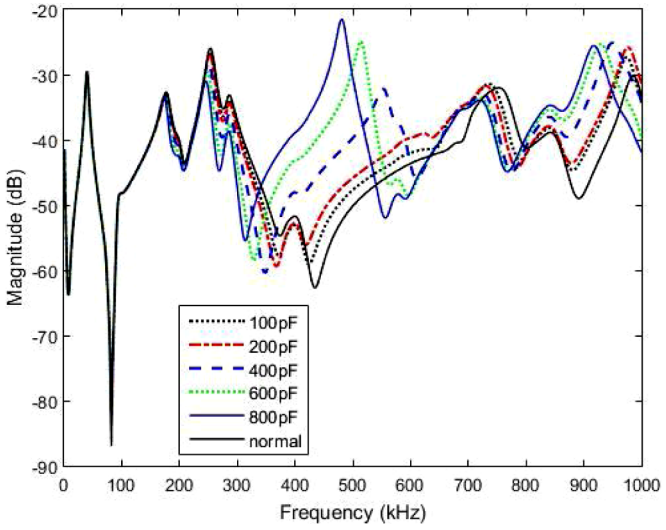

Fig. 11. Frequency response curve of different capacitances with same fault location.

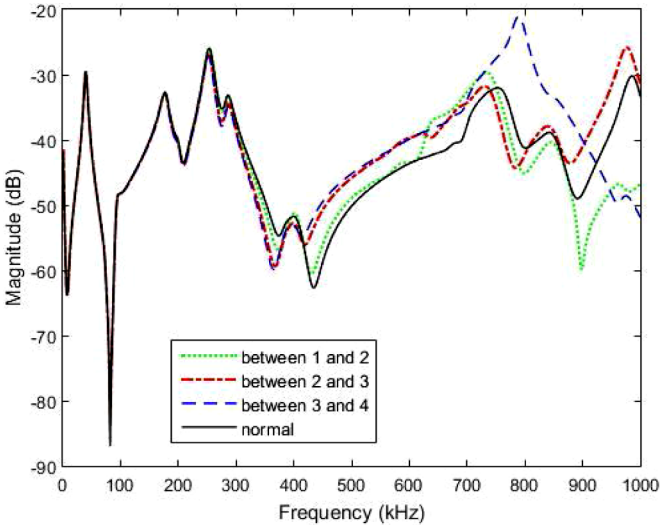

Fig. 12. Frequency response curve of the same capacitance with different fault location.

4. Frequency response analysis based on mathematical statistical indicators

Winding deformation has different effects on different frequency bands of frequency response. The deformation type of the winding can be determined preliminarily by discriminating the frequency ranges of FRA curves variation. For a more accurate judgment of the winding fault, the experimental FRA data were analyzed from the perspective of mathematical statistics. The independent variables of the above experimental groups can be roughly divided into two categories, the fault degree and the fault location. However, it does not have much practical significance to quantify the location of each fault since the processing technique based on the mathematical statistics needs to quantify the independent variables of each experimental group. As a consequence, only the experimental group corresponding to the fault degree as the independent variable is analyzed below.

4.1. Common mathematical statistical indicator

Many literatures have studied the analysis of frequency response curves with mathematical statistical indicators, and some indicators are proposed [23,34]. Commonly used mathematical statistical indicators for FRA spectrum analysis can be divided into two categories, one is extracted directly from FRA amplitude vector and the other is based on the resonance and anti-resonance points. In order to make the research more typical, we selected 10 indices from the first type of indicators and 6 indices from the second type. They are summarized in the Table 2 and their mathematical formulas are as follows, respectively.

$$ED = \sqrt{\sum_{i=1}^{N} [Y(i) - X(i)]^2} \tag{3}$$

$$SSRE = \frac{1}{N} \sum_{i=1}^{N} \left[\frac{Y(i)}{X(i)} - 1 \right]^2 \tag{4}$$

$$SSMMRE = \frac{1}{N} \sum_{i=1}^{N} \left\{ \frac{\max[Y(i), X(i)]}{\min[Y(i), X(i)]} - 1 \right\}^2 \tag{5}$$

$$\delta = \frac{1}{N} \sum_{i=1}^{N} \sqrt{\left\{ \frac{X(i) - [Y(i) + X(i)]/2}{[Y(i) + X(i)]/2} \right\}^2 + \left\{ \frac{Y(i) - [Y(i) + X(i)]/2}{[Y(i) + X(i)]/2} \right\}^2} \tag{6}$$

$$ID = \int [Y(f) - X(f)] df \tag{7}$$

$$IA = \int |Y(f) - X(f)| df \tag{8}$$

Table 2
Abbreviation definition of the numerical indices.

Abbreviation	Definition	References	Type
ED	Euclidean Distance	[17,24]	1
SSRE	Sum Squared Ratio Error	[17,24,25]	1
SSMMRE	Sum Squared Max-Min Ratio Error	[25]	1
δ	Spectrum deviation	[26,27]	1
ID	Integral of Difference	[28]	1
IA	Integral of Absolute difference	[23,27]	1
SDA	Standardized Difference Area	[29]	1
ALSE	Absolute Sum of Logarithmic Error	[25,30]	1
cc	Correlation Coefficient	[23,30,31]	1
ρ	Normalized correlation coefficient	[29,32]	1
IAD	Amplitude Deviation	[29,33]	2
MAD	Mean Amplitude Deviation	[32]	2
IFD	Index of Frequency Deviation	[29,33]	2
MFD	Mean Frequency Deviation	[32]	2
F_a	Amplitude Function	[34]	2
F_f	Frequency Function	[34]	2

$$SDA = \frac{\int |Y(f) - X(f)| df}{\int |X(f)| df} \tag{9}$$

$$ALSE = \frac{\sum_{i=1}^{N} [20\log_{10} Y(i) - 20\log_{10} X(i)]}{N} \tag{10}$$

$$cc = \frac{\sum_{i=1}^{N} X(i) Y(i)}{\sqrt{\sum_{i=1}^{N} [X(i)]^2 \sum_{i=1}^{N} [Y(i)]^2}} \tag{11}$$

$$\rho = \frac{\sum_{i=1}^{N} X^*(i) Y^*(i)}{\sqrt{\sum_{i=1}^{N} [X^*(i)]^2 \sum_{i=1}^{N} [Y^*(i)]^2}}$$
$$X^*(i) = |X(i)| - \frac{1}{N} \sum_{i=1}^{N} X(i)$$
$$Y^*(i) = |Y(i)| - \frac{1}{N} \sum_{i=1}^{N} Y(i) \tag{12}$$

$$IAD = \sum_{i=1}^{N} \left| \frac{A_Y(i) - A_X(i)}{A_X(i)} \right| \tag{13}$$

$$MAD = \frac{1}{N} \sum_{i=1}^{N} |A_Y(i) - A_X(i)| \tag{14}$$

$$IFD = \sum_{i=1}^{N} \left| \frac{f_Y(i) - f_X(i)}{f_X(i)} \right| \tag{15}$$

$$MFD = \frac{1}{N} \sum_{i=1}^{N} |f_Y(i) - f_X(i)| \tag{16}$$

$$F_a = \sum_{i=1}^{N} \frac{A_Y(i)}{A_X(i)} \tag{17}$$

$$F_f = \sum_{i=1}^{N} \frac{f_Y(i)}{f_X(i)} \tag{18}$$

The FRA traces are expressed as vectors of magnitude and phase with each discrete element of vector which corresponds to one frequency point [11]. In the equations above, Y and X are the magnitude vectors of the measured FRA trace and its fingerprint, respectively. $X(i)$ and $Y(i)$ are the i th elements of these vectors. f is the vector of frequency sample. $A(i)$ and $f(i)$ are the amplitude and the frequency of the i th resonance or anti-resonance, N is the number of samples in a vector .

4.2. Processing experimental data results

We calculate the mathematical statistical indicators of each group of experimental results in individual sub-frequency bands. Because this

study aims to find out the suitable mathematical statistical indicators which can best reflect the degree of each winding fault type, and there is space limitation of manuscript, the results of each mathematical statistical indicator are impossible to present one by one. In addition, the deformation fault degree of each experimental group is quantified, and the quantitative method will be explained below. Then the relationship between the calculated mathematical statistical indicators (Y) and the quantified fault degree (X) was evaluated by two indexes, namely, correlation coefficient (r) and sensitivity (S). At the same time, we are also concerned about whether the relationship between these mathematical indicators and fault degree is monotonous; another criteria index monotonicity (M) is analyzed. The formulas for calculating correlation coefficient and sensitivity are as follows.

$$r = \frac{\sum_{i=1}^{n}(X_i - \overline{X})(Y_i - \overline{Y})}{\sqrt{\sum_{i=1}^{n}(X_i - \overline{X})^2 \sum_{i=1}^{n}(Y_i - \overline{Y})^2}} \tag{19}$$

$$S = \frac{\overline{XY} - \overline{X}.\ \overline{Y}}{\overline{X^2} - (\overline{X})^2} \tag{20}$$

Correlation coefficient is the main factor for considering. It is a measure of the degree of linear correlation between fault degree and mathematical indicators. When correlation coefficient is larger than 0.8, it can be considered that there is a good linear correlation. Considering that the correlation coefficient is the key to accurately determine the degree of fault, the mathematical indicators of which the corresponding correlation coefficient is larger than 0.9 are only considered. In addition, the sensitivity index refers to the slope of the straight line, which is obtained by fitting each mathematical statistical indicator value with the quantified value of fault degree by least square method. As for the evaluation criterion of monotonicity, when a certain indicator changes monotonously with the increase of the quantified value of fault degree, the monotony is regarded as Y, otherwise it is N. When quantifying different fault types, there is no same standard, so the calculated correlation coefficient and sensitivity only have the significance by horizontal comparisons, which refer to the comparisons among the indicators in the experimental groups of same fault type.

It is necessary to calculate the specific values of each indicator in three frequency bands under various degrees of faults. The frequency response of the winding in the health condition is regarded as basis. Then we calculate the correlation coefficient and sensitivity between the quantized value of fault degree and 16 mathematical indicators, and judge the monotonicity between them. Finally, by comprehensively analyzing the correlation coefficient, sensitivity and monotonicity indexes, the most suitable mathematical statistical indicators for evaluating the fault degree are suggested for each winding fault type.

4.2.1. Winding inter-disk short circuit fault

The degree of winding inter-disk short circuit fault is defined. When the winding connector 1 and 2 are short circuited, the fault quantization value of the experiment is set as 1. When winding connectors 1 and 3 are short circuited, the fault quantization value of the experiment is set as 2, so as to the remaining three sets of experimental faults, which are quantified as 3, 4, and 5, respectively. The calculation results of obtained correlation coefficient, sensitivity and monotonicity indexes are shown in Tables 3–5 of the Appendix.

After analyzing the data in the three tables, it is found that for winding inter-disk short circuit fault, the best frequency band to analyze is the low frequency band. Because the indicators of the low frequency bands and the fault degree have a high linear correlation, while the linear correlation of the indicators in the middle and high frequency bands is not as good as those of the low frequency bands. Furthermore, with the disappearance of the resonance or the occurrence of a new resonance, it is difficult to calculate the statistical indicators based on the resonant point in the middle or high frequency bands.

Table 3
The evaluation index of individual mathematical indicators of FRA under winding short circuit fault in low frequency range.

Index	ED	SSRE	SSMMRE	δ	ID
r	0.9982	0.9780	0.9961	0.9973	0.9992
S	11.830	0.140	0.013	0.024	131.230
M	Y	Y	Y	Y	Y

Index	IA	ALSE	CC	ρ	IAD
r	0.9973	−0.9990	−0.9981	−0.9789	0.9998
S	12.010	−0.337	−0.004	−0.024	0.912
M	Y	Y	Y	Y	Y

Index	MAD	IFD	MFD	F_a	F_f
r	0.9927	0.9823	0.9820	−0.9894	0.9816
S	0.988	0.187	0.375	−0.059	0.188
M	Y	Y	Y	Y	Y

Table 4
The evaluation index of individual mathematical indicators of FRA under winding short circuit fault in medium frequency range.

Index	ED	SSRE	SSMMRE	δ	ID
r	0.8702	0.6133	0.8334	0.8712	0.9071
S	86.205	0.2124	0.0366	0.0609	1672.22
M	N	N	N	N	N

Index	IA	ALSE	CC	ρ	IAD
r	0.8980	−0.8621	−0.7355	−0.9317	×
S	1559.2	−0.8065	−0.0152	−0.3618	×
M	N	N	N	N	×

Index	MAD	IFD	MFD	F_a	F_f
r	×	×	×	×	×
S	×	×	×	×	×
M	×	×	×	×	×

Table 5
The evaluation index of individual mathematical indicators of FRA under winding short circuit fault in high frequency range.

Index	ED	SSRE	SSMMRE	δ	ID
r	0.8907	0.8501	0.9153	0.9243	0.9712
S	86.205	0.241	0.0502	0.088	2208.4
M	N	N	N	N	Y

Index	IA	ALSE	CC	ρ	IAD
r	0.9207	−0.9613	−0.3351	−0.5339	×
S	1425.7	−1.550	−0.005	−0.1577	×
M	N	Y	N	N	×

Index	MAD	IFD	MFD	F_a	F_f
r	×	×	×	×	×
S	×	×	×	×	×
M	×	×	×	×	×

In the low frequency band, each indicator has a good linear correlation with the fault degree. Among all the indicators, the *ALSE, cc,* ρ and F_a are negatively correlated with the fault degree, while the indicators such as *ED, ID* and *IA* are positively correlated with the fault degree, the sensitivity is high, and therefore, these indicators may be more suitable for analysis of winding short circuit fault. The calculated *ED, ID* and *IA* of short circuit fault FRA curves in low frequency band are shown in Fig. 13.

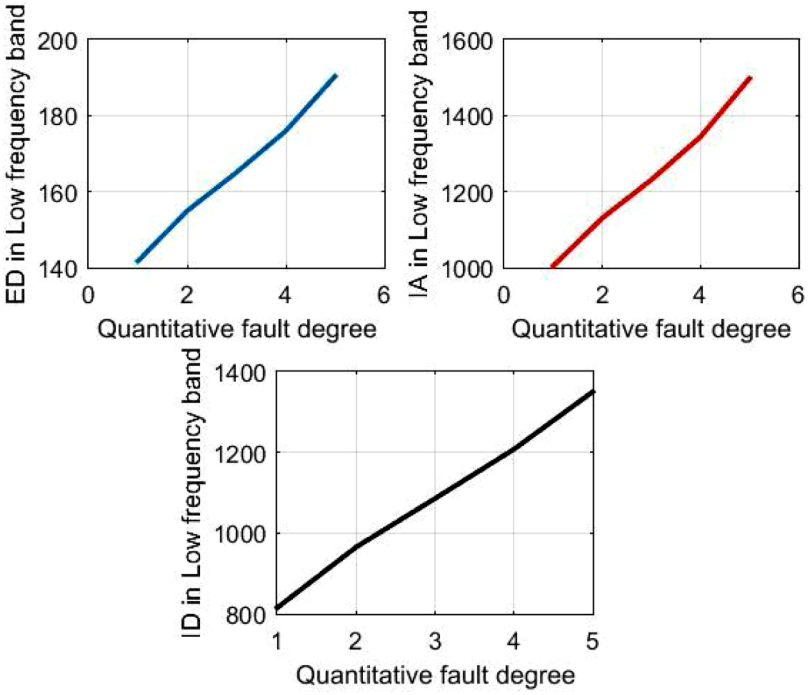

Fig. 13. *ED* in low frequency band, *IA* in low frequency band and *ID* in low frequency band.

4.2.2. Winding radial deformation fault

In this group of experiment, the extent of winding radially deformed part is regarded as the quantitative value of the fault degree. The calculation results of correlation coefficient, sensitivity and monotonicity indexes for each mathematical indicator are shown in Tables 6–8 in the Appendix.

From the three tables, it can be found that the mathematical indicators with corresponding linear correlation coefficient larger than 0.9 include *IAD* in the middle frequency band, and *MFD, F_f* in the high frequency band. Fig. 14 shows the change of mathematical indicators in the specific frequency band when various radial deformations take place in the winding. The curves of *MFD* and F_f are not linear; there exist the kink in the diagrams. In Fig. 9, it can be found that within 600~1000 kHz, the shift of resonance point along x-axis does not increase linearly with the increase of fault degree, which may be the reason why the curves based on these two indicators have kinks in the high frequency band, because the curves are based on the frequency offset of the resonant point. The above phenomenon might be due to the impact of RD fault on the equivalent electrical parameter is not linear.

Table 7
The evaluation index of individual mathematical indicators of FRA under winding radial deformation fault in medium frequency range.

Index	ED	SSRE	SSMMRE	δ	ID
r	−0.0673	0.1347	0.1291	0.0489	0.2446
S	41.429	0.004	0.003	0.014	2374.3
M	N	N	N	N	N
Index	IA	ALSE	CC	ρ	IAD
r	0.040	−0.2471	−0.1202	−0.1214	0.9218
S	383.24	−0.850	−0.002	−0.045	1.504
M	N	N	N	N	Y
Index	MAD	IFD	MFD	F_a	F_f
r	−0.4741	0.3208	−0.3714	0.6317	−0.4256
S	−4.426	0.2361	−12.167	1.204	−0.251
M	N	N	N	N	N

Table 6
The evaluation index of individual mathematical indicators of FRA under winding radial deformation fault in low frequency range.

Index	ED	SSRE	SSMMRE	δ	ID
r	0.3746	0.2146	0.2268	0.1767	−0.6762
S	189.850	0.011	0.008	0.041	−117.18
M	N	N	N	N	N
Index	IA	ALSE	CC	ρ	IAD
r	0.2165	0.7877	−0.255	−0.2451	0.7637
S	471.41	−0.1430	−0.011	−0.223	1.033
M	N	N	Y	N	N
Index	MAD	IFD	MFD	F_a	F_f
r	−0.8783	0.599	−0.4214	0.8960	−0.5986
S	−37.30	1.270	−5.919	1.258	−1.270
M	N	N	N	N	N

Table 8
The evaluation index of individual mathematical indicators of FRA under winding radial deformation fault in high frequency range.

Index	ED	SSRE	SSMMRE	δ	ID
r	−0.2389	0.2230	−0.2477	−0.2967	0.3190
S	−109.77	−0.006	−0.006	−0.089	4300.8
M	N	N	N	N	N
Index	IA	ALSE	CC	ρ	IAD
r	−0.2775	−0.3180	0.2279	0.3502	−0.3003
S	−1921.5	−2.285	0.001	0.082	−0.2048
M	N	N	N	N	N
Index	MAD	IFD	MFD	F_a	F_f
r	0.2138	−0.8037	−0.9042	−0.1810	−0.9166
S	5.4187	−0.086	−45.421	−0.5574	−0.2568
M	N	N	N	N	Y

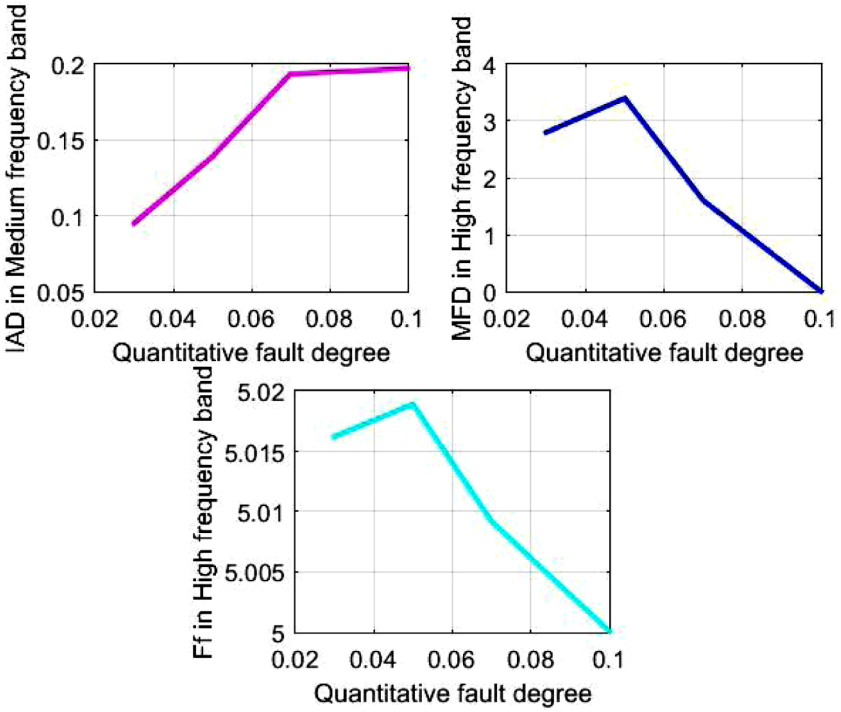

Fig. 14. *IAD* in medium frequency band, *MFD* in high frequency band and F_f in high frequency band.

As degree of RD fault increase, both the inductance and capacitance parameter change, winding inductance is increasing, while some winding capacitance parameters are decreasing, as a result, the resonant point changes. However, thecurve of *IAD* is approximately linear. The ideal indicator for diagnosing the fault degree of radial deformation is *IAD*, because *MFD* and F_f are negatively correlated with the fault degree and there is no monotonicity between the two indicators and the quantified value of fault severity. Besides, it is also found that the best frequency band for analyzing winding radial deformation fault is the middle frequency range. Moreover, it probably can be concluded that the second type of mathematical indicator based on resonant frequency, namely the *IAD* (middle frequency band), is more suitable for analyzing the fault degree of radial deformation fault, based on the experimental FRA data.

4.2.3. Disk space variation fault

In this experiment, the value of paralleled capacitance is regarded as the fault degree of disk space variation fault. The obtained calculation results of correlation coefficient, sensitivity and monotonicity indexes for each mathematical indicator are shown in Tables 9–11 in the Appendix.

From the three tables, it can be found that the mathematical statistical indicators in the middle frequency band have a good linear correlation with the fault degree, thus, the mathematical statistical indicators of middle frequency band is suitable for diagnosing the disk space variation fault. The second type of mathematical indicators based on the resonance is not easily and directly used in high frequency band because variable resonant point disappears or the new resonance points are generated. In summary, *ID* and *IA* are the most suitable mathematical statistical indicators for the degree of disk space variation fault, the calculated *ID* and *IA* of FRA curve corresponding to fault degree in the middle frequency band are shown in Fig. 15.

5. Conclusion and future work

Transformer winding deformation fault experiments were emulated on a model transformer. The characteristics of measured FRA traces

Table 9
The evaluation index of individual mathematical indicators of FRA under disk space variation fault in low frequency range.

Index	ED	SSRE	SSMMRE	δ	ID
r	0.9176	0.8915	0.8726	−0.4439	0.5444
S	0.0057	1.7×10^{-7}	1.4×10^{-7}	6.0×10^{-7}	0.0044
M	N	N	N	N	N

Index	IA	ALSE	CC	ρ	IAD
r	−0.1593	−0.1892	−0.9127	−0.8981	0.6352
S	−0.0019	2.0×10^{-6}	-2×10^{-7}	-3×10^{-7}	2.7×10^{-5}
M	N	N	N	N	N

Index	MAD	IFD	MFD	F_a	F_f
r	0.6516	0.6609	−0.8512	−0.6483	−0.6609
S	8.8×10^{-4}	1.4×10^{-4}	-7×10^{-4}	-3×10^{-5}	1.4×10^{-4}
M	N	N	Y	N	N

Table 10
The evaluation index of individual mathematical indicators of FRA under disk space variation fault in medium frequency range.

Index	ED	SSRE	SSMMRE	δ	ID
r	0.9830	0.9262	0.9579	0.9838	0.9820
S	0.2397	5.8×10^{-5}	2.9×10^{-5}	1.0×10^{-4}	1.473
M	N	N	N	N	N

Index	IA	ALSE	CC	ρ	IAD
r	0.9837	−0.9839	−0.9465	−0.9422	0.9848
S	3.3537	-5×10^{-4}	-2×10^{-5}	-7×10^{-7}	9.4×10^{-4}
M	N	N	N	N	N

Index	MAD	IFD	MFD	F_a	F_f
r	0.9594	0.9724	−0.9751	−0.9422	−0.9731
S	0.004	2.0×10^{-4}	−0.011	-4×10^{-4}	-2×10^{-4}
M	Y	N	N	Y	N

Table 11
The evaluation index of individual mathematical indicators of FRA under disk space variation fault in high frequency range.

Index	ED	SSRE	SSMMRE	δ	ID
r	0.1284	0.3662	0.3729	0.7332	−0.6939
S	0.0121	6.7×10^{-6}	6.8×10^{-6}	4.6×10^{-5}	−1.1878
M	N	N	N	N	N

Index	IA	ALSE	CC	ρ	IAD
r	0.7076	0.7392	0.2125	0.1677	×
S	1.090	6.2×10^{-4}	3.2×10^{-4}	8.0×10^{-5}	×
M	N	N	N	N	×

Index	MAD	IFD	MFD	F_a	F_f
r	×	×	×	×	×
S	×	×	×	×	×
M	×	×	×	×	×

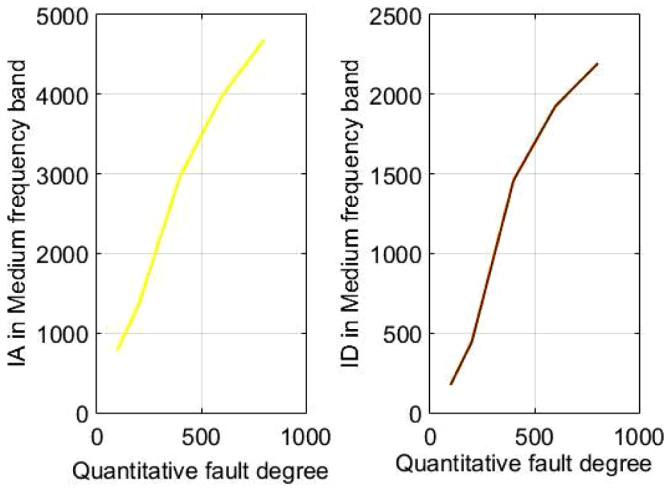

Fig. 15. *IA* and *ID* in middle frequency band.

were analyzed in three sub-frequency bands. 16 Mathematical statistical indicators of two FRA traces of normal and failure conditions were calculated. The sensitivity, relativity and monotonicity index of each indicator were used as the criteria to evaluate the applicability of mathematical indicators. The following conclusions can be derived.

1) For winding inter-disk short circuit fault, the low frequency band is the most suitable frequency band for mathematical statistical indicators analysis, and the *ED, ID* and *IA* are suggested as the indicators for fault degree diagnosis.
2) For the winding radial deformation fault, the second type of indicators based on the resonance and anti-resonance is more suitable for the analysis of the radial deformation fault, and the *IAD* is suggested as the suitable indicator.
3) For the winding disk space variation fault, the frequency band which is suitable for mathematical statistical indicator analysis is the middle frequency band, and the suitable indicators for diagnosing the fault degree are suggested as *IA* and *ID*.
4) Due to the limitation of experimental condition, these conclusions are derived from a single transformer type/connection design, the approach maybe insufficient generalization, which should be verified in some other transformers of different ratings and structures.
5) Although, there still exist some problems, the results of this study may still provide guidance for the field application of frequency response analysis.

Declaration of Competing Interest

The authors declare that they have no known competing financial interests or personal relationships that could have appeared to influence the work reported in this paper.

Acknowledgments

This work was supported in part by the Natural Science Foundation of Chongqing (cstc2019jcyj-msxmX0236), the Venture and Innovation Support Program for Chongqing Overseas Returnees (cx2019123) and the National Natural Science Foundation of China (51807166).

Appendix

Tables 3–11

References

[1] F. Yang, S. Ji, Y. Liu, F. Zhang, Research of sweep frequency impedance to determine transformer winding deformation after short-circuit impact, 2016 IEEE International Power Modulator and High Voltage Conference (IPMHVC), IEEE, 2016, July, pp. 68–72.
[2] C. Cao, X. Lin, X. Li, Research on online monitoring of transformer winding deformation state based on short circuit reactance, 2016 China International Conference on Electricity Distribution (CICED), IEEE, 2016, August, pp. 1–4.
[3] M. Bagheri, M.S. Naderi, T. Blackburn, Advanced transformer winding deformation diagnosis: moving from off-line to on-line, IEEE Trans. Dielectr. Electr. Insul. 19 (6) (2012) 1860–1870.
[4] Z. Zhao, C. Yao, X. Zhao, N. Hashemnia, S. Islam, Impact of capacitive coupling circuit on online impulse frequency response of a power transformer, IEEE Trans. Dielectr. Electr. Insul. 23 (3) (2016) 1285–1293.
[5] H. Rahbarimagham, H.K. Porzani, M.S.A. Hejazi, M.S. Naderi, G.B. Gharehpetian, Determination of transformer winding radial deformation using UWB system and hyperboloid method, IEEE Sens. J. 15 (8) (2015) 4194–4202.
[6] A. Abu-Siada, S. Islam, A novel online technique to detect power transformer winding faults, IEEE Trans. Power Delivery 27 (2) (2012) 849–857.
[7] Z. Zhao, C. Tang, Q. Zhou, L. Xu, Y. Gui, C. Yao, Identification of power transformer winding mechanical fault types based on online IFRA by support vector machine, Energies 10 (12) (2017) 2022.
[8] N. Hashemnia, A. Abu-Siada, S. Islam, Improved power transformer winding fault detection using fra diagnostics – part 1: axial displacement simulation, IEEE Trans. Dielectr. Electr. Insul. 22 (1) (2015) 556–563.
[9] S.D. Mitchell, J.S. Welsh, Modeling power transformers to support the interpretation of frequency-response analysis, IEEE Trans. Power Delivery 26 (4) (2011) 2705–2717.
[10] A. Abu-Siada, M.I. Mossad, M.F. El-Naggar, Estimating power transformer high frequency model parameters using frequency response analysis, IEEE Trans. Power Delivery (2019).
[11] M.H. Samimi, S. Tenbohlen, FRA interpretation using numerical indices: state-of-the-art, Int. J. Electr. Power Energy Syst. 89 (2017) 115–125.
[12] A. Abu-Siada, O. Aljohani, Detecting incipient radial deformations of power transformer windings using polar plot and digital image processing, IET Sci. Measure. Tech. 12 (4) (2018) 492–499.
[13] N. Hashemnia, A. Abu-Siada, S. Islam, Improved power transformer winding fault detection using FRA diagnostics–part 2: radial deformation simulation, IEEE Trans. Dielectr. Electr. Insul. 22 (1) (2015) 564–570.
[14] Z.W. Zhang, W.H. Tang, T.Y. Ji, Q.H. Wu, Finite-element modeling for analysis of radial deformations within transformer windings, IEEE Trans. Power Delivery 29 (5) (2014) 2297–2305.
[15] M. Bigdeli, M. Vakilian, E. Rahimpour, Transformer winding faults classification based on transfer function analysis by support vector machine, IET Electr. Power Appl. 6 (5) (2012) 268–276.
[16] O. Aljohani, A. Abu-Siada, Application of digital image processing to detect short-circuit turns in power transformers using frequency response analysis, IEEE Trans. Ind. Inf. 12 (6) (2016) 1–2.
[17] A.J. Ghanizadeh, G.B. Gharehpetian, ANN and cross-correlation based features for discrimination between electrical and mechanical defects and their localization in transformer winding, IEEE Trans. Dielectr. Electr. Insul. 21 (5) (2014) 2374–2382.
[18] E. Rahimpour, M. Jabbari, S. Tenbohlen, Mathematical comparison methods to assess transfer functions of transformers to detect different types of mechanical faults, IEEE Trans. Power Delivery 25 (4) (2010) 2544–2555.
[19] Z. Zhao, C. Yao, C. Li, S. Islam, Detection of power transformer winding deformation using improved FRA based on binary morphology and extreme point variation, IEEE Trans. Indust. Electron. 65 (4) (2017) 3509–3519.
[20] E. Gomez-Luna, G.A. Mayor, C. Gonzalez-Garcia, J.P. Guerra, Current status and future trends in frequency-response analysis with a transformer in service, IEEE Trans. Power Delivery 28 (2) (2013) 1024–1031.
[21] A. Abu-Siada, N. Hashemnia, S. Islam, M.A. Masoum, Understanding power transformer frequency response analysis signatures, IEEE Electr. Insul. Mag. 29 (3)

(2013) 48–56.
[22] Frequency response analysis on winding deformation of power transformers, People Republic of China, Electric Power Industry Standard, DL/T911-2004, ICS27.100, F24, Document No. 15182-2005, 2005.
[23] Measurement of frequency response, IEC Standard 60076-18, Ed. 1.0, 2012–07.
[24] K. Pourhossein, G.B. Gharehpetian, E. Rahimpour, B.N. Araabi, A probabilistic feature to determine type and extent of winding mechanical defects in power transformers, Elect. Pow. Syst. Res. 82 (1) (2012) 1–10.
[25] J.W. Kim, B. Park, S.C. Jeong, S.W. Kim, P. Park, Fault diagnosis of a power transformer using an improved frequency-response analysis, IEEE Trans. Power Delivery 20 (1) (2005) 169–178.
[26] W.H. Tang, A. Shintemirov, Q.H. Wu, Detection of minor winding deformation fault in high frequency range for power transformer, IEEE PES general meeting, IEEE, 2010, July, pp. 1–6.
[27] T.Y. Ji, W.H. Tang, Q.H. Wu, Detection of power transformer winding deformation and variation of measurement connections using a hybrid winding model, Elect. Pow. Syst. Res. 87 (2012) 39–46.
[28] M. Wang, A.J. Vandermaar, K.D. Srivastara, Evaluation of frequency response analysis data, 14th international symposium on high voltage engineering, 2001, August, pp. 904–907.
[29] V. Behjat, M. Mahvi, Statistical approach for interpretation of power transformers frequency response analysis results, IET Sci. Measure. Tech. 9 (3) (2015) 367–375.
[30] P.M. Nirgude, D. Ashokraju, A.D. Rajkumar, B.P. Singh, Application of numerical evaluation techniques for interpreting frequency response measurements in power transformers, IET Sci. Measure. Tech. 2 (5) (2008) 275–285.
[31] J.C.G. Arispe, E.E. Mombello, Detection of failures within transformers by fra using multiresolution decomposition, IEEE Trans. Power Delivery 29 (3) (2014) 1127–1137.
[32] R. Wimmer, S. Tenbohlen, M. Heindl, A. Kraetge, M. Krüger, J. Christian, Development of algorithms to assess the FRA, Proceedings of 15th Int. Symp. High Voltage Engineering, Ljubljana, Slovenia, 2007, August.
[33] P.M. Nirgude, D. Ashokraju, A.D. Rajkumar, B.P. Singh, Application of numerical evaluation techniques for interpreting frequency response measurements in power transformers, IET Sci. Measure. Tech. 2 (5) (2008) 275–285.
[34] R.K. Senobari, J. Sadeh, H. Borsi, Frequency response analysis (FRA) of transformers as a tool for fault detection and location: a review, Elect. Pow. Syst. Res. 155 (2018) 172–183.